INTERNATIONAL JOURNAL OF OPTIMIZATION IN CIVIL ENGINEERING
Int. J. Optim. Civil Eng., 2015; 5(3):353-374

A NEW HYBRID ALGORITHM FOR TOPOLOGY OPTIMIZATION OF DOUBLE LAYER GRIGS

M. Mashayekhi[1], E. Salajegheh[2*, †] and M. Dehghani[1]
[1]*Department of Civil Engineering, Vali-e-Asr University of Rafsanjan, Iran*
[2]*Department of Civil Engineering, Shahid Bahonar University of Kerman, 76169-133, Iran*

ABSTRACT

In this paper, for topology optimization of double layer grids, an efficient optimization method is presented by combination of Imperialist Competitive Algorithm (ICA) and Gravitational Search Algorithm (GSA) which is called ICA-GSA method. The present hybrid method is based on ICA but the moving of countries toward their relevant imperialist is done using the law of gravity of GSA. In topology optimization process, the weight of the structure is minimized subjected to displacements of joints, internal stress and slenderness ratio of members constraints. Through numerical example, topology optimization of a typical large-scale double layer grid is obtained by ICA, GSA and ICA-GSA methods. The numerical results indicate that the proposed algorithm, ICA-GSA, executes better than ICA, GSA and the other methods presented in the literatures for topology optimization of large-scale skeletal structures.

Keywords: double layer grids; topology optimization; gravitational search algorithm; imperialist competitive algorithm.

Received: 25 March 2015; Accepted: 22 June 2015

1. INTRODUCTION

Optimization of truss structures has been one of the most active fields of research for many years in the field of optimization algorithms and applications in engineering [1 and 2]. In general, truss optimizations can be categorized into three classes: (1) sizing optimization, where cross-sectional areas of members (elements) are considered as design variables, while the structural geometry is fixed; (2) geometry optimization, where joint coordinates are design variables, while the connections (elements) of nodes are fixed [3]; and (3) topology

[*]Corresponding author: Department of Civil Engineering, Shahid Bahonar University of Kerman, Iran
[†]E-mail address: eysasala@mail.uk.ac.ir (E. Salajegheh)

optimization, where the connections of nodes are design variables [4 and 5]. Many researches are a combination of these three types of optimization [6]. Many techniques have been reformed to search optimal truss structures. Classical optimization methods, such as the branch-and-bound algorithm [7], were first employed. However, various recently developed methods use evolutionary computations to solve truss optimization problems, such as genetic algorithms [8 and 9], particle swarm optimization [10], simulated annealing algorithms [11], ant colony optimization [12 and 13] and artificial bee colony algorithms [14]. A major difficulty in solving truss topology optimization is that some structures may represent a singular point in the given search space [15-17]. Kirsch (1989) [5], shows some analytical conditions, such as loading conditions and structure stability, to gain optimal geometries. Su *et al.* (2009) [18], used two different matrices to present the cross-sectional areas and the existence of members. A random number is generated to decide the value of each topological bit in the individuals in the initial generation. Deb and Gulati (2001) [2], presented a new methodology to introduce the existence of members so that the cross-sectional areas and topology variables can be optimized simultaneously. Truss optimization is also complex, and involves various constraints, such as stress, displacement, frequency, slenderness ratio, reliability and buckling [19].

Space structures, as large-scale skeletal structures, belong to specific class of three dimensional structures with special configurations. These structures are broadly used to cover large areas without intermediate columns. Space structures are often categorized as grids, domes and barrel vaults [20]. Double layer grids are classical cases of prefabricated space structures and also the most popular forms which are frequently used nowadays.

In topology optimization of large-scale skeletal structures with discrete cross-sectional areas, if the heuristic optimization algorithms are combined with continuous-based topology optimization methods, their performance can be increased. For example, a two-stage optimization method for reliability-based topology optimization of double layer grid has been introduced by Mashayekhi *et al.* [21] which has been performed by employing the Methods of Moving Asymptotes (MMA) and Ant Colony Optimization (ACO). Also, an ESO-ACO method has been presented by Mashayekhi *et al.* [22] which consists of the Evolutionary Structural Optimization (ESO) and Ant Colony Optimization for minimizing the weight of double layer grids while artificial ground motion is used to calculate the structural dynamic responses. Furthermore, to achieve Reliability-Based Topology Optimization (RBTO) of double layer grids, Mashayekhi *et al.* [23] have introduced SIMP-ACO method.

In this paper, for topology optimization of double layer grids, an efficient optimization method is introduced by combination of ICA and GSA which is denominated ICA-GSA method. The present combined method is based on ICA but it uses the law of gravity of GSA to move countries toward their relevant imperialist. The numerical results show the computational advantages of the proposed ICA-GSA method to search the optimum topology of large-scale skeletal structures.

2. TOPOLOGY OPTIMIZATION OF DOUBLE LAYER GRIDS

In topology optimization of double layer grids, the presence or absence of the bottom joints (nodes) and also the cross-sectional areas are chosen as design variables while the support

locations and the coordinates of nodes are kept fixed. The symmetry properties of the structure are used to tabulate the joints which cause to decrease in the design space. Therefore, the joints are deleted in groups of 8, 4 or 1 [21]. Also, a variable (topology variable) is used to determine the presence or absence of each joint group which takes the value of 1 and 0 for the two cases, respectively. The *i*th node group should be removed from the ground structure if the *i*th topology variable takes a zero value [21]. In the double layer grids topology optimization, the number of design variables (*NDV*) is summation of the number of topology variables (*NTV*) and the number of compressive and tensile element types [21].

Discrete variables are used to determine the suitable cross-sectional area of the structural members. These variables are selected from the available pipe profiles, with specified thickness and outer diameter. To stay unchanged the load bearing areas of top layer joints, and also to obtain a practical structure, the existence of nodes in the top grid is not considered as a variable [21].

In topology optimization of the double layer grids to minimize the weight of the structure (*W*), the optimum amounts of the design variables are searched under constraints on stress (g_σ), slenderness ratio (g_λ) and displacement (g_δ) [21]:

$$\begin{aligned} &\textit{Find}: \overline{\mathbf{A}} = [J_1, J_2, ..., J_{NTV}, a_1, a_2, ..., a_{NMG}]^T \\ &\qquad J_i \in [0,1], \quad i = 1, 2, ..., NTV \\ &\qquad a_k \in \tilde{\mathbf{A}}, \quad k = 1, 2, ..., NMG \\ &\textit{to minimize}: \; W = \rho^e \sum_{k=1}^{NMG} a_k \sum_{i=1}^{N_k} l_i \\ &\textit{subject to}: \qquad g_\sigma, g_\lambda, g_\delta \le 0 \end{aligned} \tag{1}$$

where *NMG* is the number of member groups, J_i is the *i*th topology variable, N_k is the number of members in the *k*th member group, a_k is the discrete cross-sectional area of the *k*th member group which is chosen from steel pipes in an available profile list ($\tilde{\mathbf{A}}$), ρ^e is the material density and l_i is the length of the *i*th element. It is noted that in topology optimization process, if an unstable structure is recognized, new random values are consecutively generated only for its topology variables, until a stable structure is achieved [21]. Therefore, all of the structures that their objective function is calculated using (1) are stable and it is not necessary to allocate a penalty to unstable ones.

To solve a constrained optimization problem, its objective function should be reformed in such a way that the constrained problem should be converted to an unconstrained one. Thus, only one modified objective function (Ψ) is minimized [24]. In this paper, Ψ is defined as [21]:

$$\Psi(\overline{\mathbf{A}}) = \mathrm{W}(\overline{\mathbf{A}})(1 + \mathrm{Co}(\overline{\mathbf{A}}))^2 \tag{2}$$

in which

$$Co(\overline{\mathbf{A}}) = \sum_{i=1}^{ne} (g_{\sigma,i}(\overline{\mathbf{A}}) + g_{\lambda,i}(\overline{\mathbf{A}})) + \sum_{j=1}^{nj} g_{\delta,i}(\overline{\mathbf{A}}) \tag{3}$$

where *Co* is the penalty function, *ne* is the number of elements and *nj* is the number of nodes (joints).

3. GRAVITATIONAL SEARCH ALGORITHM (GSA)

Gravitational search algorithm (GSA) is based on the law of gravity [25]. In this algorithm, agents are considered as objects and their fitness is considered as their masses. All these masses attract each other by the gravity force, and this force causes a global displacement of all masses toward the heavier ones. The heavy masses corresponding to the proper answers move more slowly than lighter ones. In GSA, the *i*th mass (agent) has four characteristics: position ($\mathbf{X}_i$), inertial mass (M_i), active gravitational mass (M_{ai}), and passive gravitational mass (M_{pi}). Now, consider a system with N agents (masses). The position of the *i*th agent is determined as follows [25]:

$$\mathbf{X}_i(t) = (x_i^1(t), ..., x_i^d(t), ..., x_i^n(t)), i = 1, 2, ..., N \tag{4}$$

where $x_i^d(t)$ is the position of the *i*th agent in the *d*th dimension at the *t*th time. The acceleration acting on the *i*th mass is calculated as follows [25]:

$$a_i^d(t) = \sum_{j=1, j\neq i}^{n} rand_j G(t) \frac{M_{aj}(t)}{R_{ij}(t) + \varepsilon} (x_i^d(t) - x_j^d(t)) \tag{5}$$

where $rand_j$ is a random number in the interval [0,1], $R_{ij}(t)$ is the Euclidian distance between two agents *i* and *j*, G is the gravitational constant which is assumed at the beginning and decreases in the *t*th time to control the search accuracy, and ε is a small constant. Furthermore, the next velocity of an agent is considered as a fraction of its current velocity added to its acceleration. Therefore, its velocity and its position are calculated as follows [25]:

$$v_i^d(t+1) = rand_i \times v_i^d(t) + a_i^d(t) \tag{6}$$

$$x_i^d(t+1) = x_i^d(t) + v_i^d(t+1) \tag{7}$$

where $rand_i$ is a uniform random variable in the interval [0,1]. This random number is used to give a randomized characteristic to the search. The gravitational and inertia masses are simply calculated by the fitness evaluation as follows [25]:

$$m_i(t) = \frac{fit_i(t) - worst(t)}{best(t) - worst(t)} \tag{8}$$

$$M_i(t) = \frac{m_i(t)}{\sum_{j=1}^{N} m_j(t)} \tag{9}$$

$$M_{pi} = M_{ai} = M_i, i = 1, 2, ..., N \tag{10}$$

where $fit_i(t)$ is the fitness value of the *i*th agent at the *t*th time and for a minimization problem worst(t) and best(t) are defined as follows:

$$\text{best}(t) = \min\left[\text{fit}_j(t), j \in \{1,...,N\}\right] \tag{11}$$

$$\text{worst}(t) = \max\left[\text{fit}_j(t), j \in \{1,...,N\}\right] \tag{12}$$

To have discrete results, a rounding function is employed which converts the magnitude of a result to the nearest discrete value, as follows:

$$x_i^d(t+1) = \text{Round}(x_i^d(t+1)) \tag{13}$$

where Round is a function that rounds a result to the nearest integer neighbor.

4. IMPERIALIST COMPETITIVE ALGORITHM (ICA)

ICA, which is introduced by Atashpaz *et al*. [26], is inspired from the socio-political process of imperialism and imperialistic competition, and is applied to structural optimization by Kaveh and Talatahari [27]. ICA initiates with a primary population. Each individual of the population is called a 'country'. Some of the best countries, with the minimum cost, are considered as the imperialist states and the rest will be the colonies of those imperialist states. All the colonies are divided among the imperialist countries proportional to their power. In addition, the main ICA segments are briefly described [26]:

4.1 Creation of initial empires

In ICA each point of the design space is identified as a country. In an N_{var}-dimensional optimization problem, the *i*th country is a $1 \times N_{var}$ array. This array is determined as follow [26]:

$$country_i = \left[p_1^i, ..., p_d^i, ..., p_{N_{var}}^i\right] \tag{14}$$

where p_d^i is the position of the *i*th country in the *d*th dimension.

The cost of a country is found by evaluation of the cost function (*f*) of variables. So we have [26]:

$$c_i = cost_i = f\,(country_i) = f\,(p_1^i, ..., p_d^i, ..., p_{N_{var}}^i) \tag{15}$$

To start the optimization process, initial countries of size $N_{Country}$ is produced and some of the most powerful countries (N_{imp}) are selected to form the empires. The remaining N_{col} of the initial countries are divided among imperialists based on their power. To proportionally divide the colonies among imperialists, the normalized cost of an imperialist is identified by [26]:

$$C_n = \max_i \{c_i\} - c_n \tag{16}$$

where c_n is the cost of the nth imperialist and C_n is its normalized cost. Having the normalized cost of all imperialists, the normalized power of each imperialist is calculated by [26]:

$$P_n = \left| \frac{C_n}{\sum_{i=1}^{N_{imp}} C_i} \right| \tag{17}$$

The initial colonies are divided among empires based on their power. Then, the number of colonies of the nth empire ($N.C_n$) will be:

$$N.C_n = round\left\{P_n \times N_{col}\right\} \tag{18}$$

To divide the colonies, $N.C_n$ of the colonies is randomly chosen and is given to the nth imperialist [26].

4.2 Movement of the colonies toward their imperialist

In the ICA, the assimilation policy is modeled by moving all the colonies toward their imperialist. This movement is shown in Fig. 1 in which a colony moves toward the imperialist by x units. The new position of colony is shown in a darker color. The direction of the movement is the vector from the colony to the imperialist. In this figure, x is a random number with uniform distribution. Then [26]:

$$x \sim U\left(0, \beta \times d\right), \beta > 1 \tag{19}$$

where β is a number greater than one and d is the distance between the colony and the imperialist situation. $\beta > 1$ causes the colonies to get closer to the imperialist state from both sides.

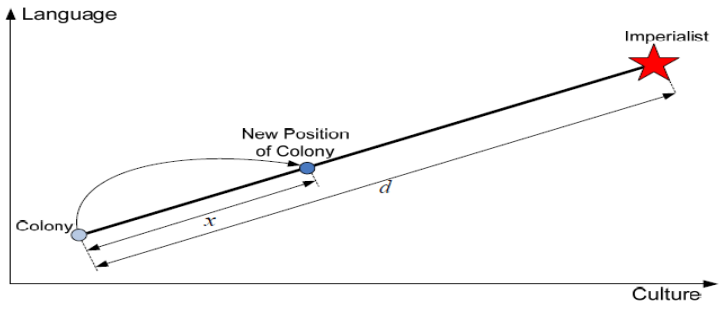

Figure 1. The movement of a colony toward its imperialist [26]

4.3 Exchanging the imperialist with a powerful colony

While moving toward the imperialist, a colony might reach to a location with lower cost

than the imperialist. In this case, the imperialist and the colony change their positions. Then, the algorithm will continue by the imperialist in the new position [26].

4.4 Total power of an empire

Total power of an empire is influenced by the power of imperialist country. However, the power of the colonies of an empire has an effect on the total power of that empire. This fact is considered by defining the total cost of an empire by [26]:

$$TC_n = Cost\left(imperialist_n\right) + \xi\left\{mean\left(Cost\left(colonies \quad of \quad empire_n\right)\right)\right\} \tag{20}$$

where TC_n is the total cost of the nth empire and ξ is a positive small number. A little value for ξ causes the total power of the empire to be calculated by just the imperialist and increasing it will increase to the role of the colonies in determining the total power of an empire. The value of 0.1 for ξ has shown good results in most of the executions [26].

4.5 Imperialistic competitions

All empires attempt to take the possession of colonies of other empires and control them. The imperialistic competition moderately brings about a decrease in the power of weaker empires and an increase in the power of more powerful ones. The imperialistic competition is modeled by picking one of the weakest colonies of the weakest empire and making a competition among all empires to possess this colony. Fig. 2 shows the modeled imperialistic competition. Based on their total power, in this competition, this colony will not definitely be possessed by the most powerful empires, but these empires will be more likely to possess them.

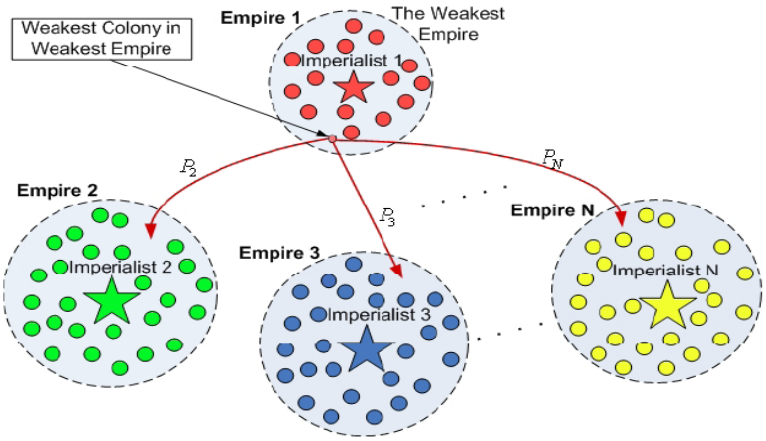

Figure 2. Imperialistic competition [26]

To start the competition, the weakest colony of the weakest empire is chosen and the possession probability of each empire is found. The possession probability (P_P) is proportionate to the total power of the empire. The normalized total cost of an empire is calculated by:

$$NTC_n = \max_i \{TC_i\} - TC_n \tag{21}$$

where TC_n and NTC_n are the total cost and the normalized total cost of the nth empire, respectively. Having the normalized total cost, the possession probability of each empire is determined by [26]:

$$P_{Pn} = \left| \frac{NTC_n}{\sum_{i=1}^{N_{imp}} NTC_i} \right| \tag{22}$$

5. A NEW HYBRID METHOD (ICA-GSA)

In ICA process, the movement of colonies is one of the important parts while in four different types of these movements are compared together [27]. In this paper, a new hybrid method is presented to improve this movement of countries toward their imperialist. In this method, in each empire, the imperialist attracts all its countries based on the gravitational law. To achieve this aim, the position of the ith colonies ($country_i$) is defined using (14), and in the jth empire, at the tth time, the gravitational acceleration of the ith country in the dth dimension ($a_i^d(t)$) is identified as follows:

$$a_i^d(t) = rand_i G(t) \frac{M_{aj}(t)}{R_{ij}(t) + \varepsilon} (p_j^d(t) - p_i^d(t)) \tag{23}$$

where $rand_i$ is a random number in the interval [0,1], $R_{ij}(t)$ is the Euclidian distance between the ith country and its imperialist (the jth imperialist), $p_j^d(t)$ is the position of the jth imperialist and M_{aj} is the active gravitational mass of the jth imperialist which is calculated in each empire as follow:

$$cc_i(t) = \frac{c_i(t) - weak(t)}{c_{imp}^j(t) - weak(t)},\ i = 1, 2, ..., N.C_j \tag{24}$$

$$M_{aj}(t) = \frac{cc_j(t)}{\sum_{i=1}^{N.C_j} cc_i(t)},\ j = 1, 2, ..., N_{imp} \tag{25}$$

In which

$$weak(t) = \max\left[c_j(t), j \in \{1, ..., N.C_j\} \right] \tag{26}$$

where c_{imp}^{j} is the cost of the *j*th imperialist.

In addition, the velocity at (*t+1*)th time and in the *d*th dimension is calculated using (6) and the new position of the *i*th country in the *d*th dimension is defined as follows:

$$p_i^d(t+1) = p_i^d(t) + v_i^d(t+1) \tag{27}$$

The flowchart of the ICA-GSA algorithm is schematically shown in Fig. 3. In this figure, reaching the number of optimization cycles to 80 is considered as a convergence criterion.

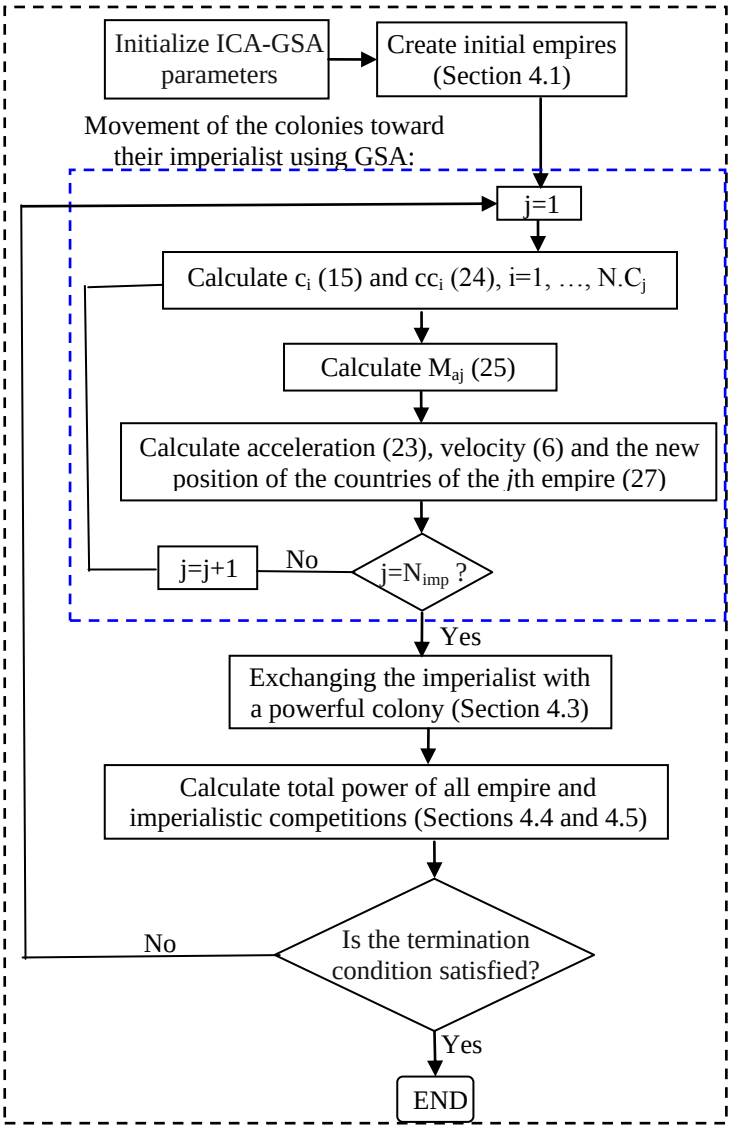

Figure 3. The flowchart of the ICA-GSA

6. NUMERICAL EXAMPLES

In order to approve the capability of the ICA-GSA, two benchmark size optimization examples are considered from the literature. These examples are considered in Sections 6.1 and 6.2. For further consideration, in Section 6.3, topology optimization of a large scale double layer grid is also studied from the literature.

6.1 A 25-bar space truss

Fig. 4 shows a 25-bar space truss. The material density is 2767.990 kg/m^3 and the modulus of elasticity is 68,950 MPa. 25 members are categorized into eight groups, as follows: (1) A1, (2) A2–A5, (3) A6–A9, (4) A10–A11, (5) A12–A13, (6) A14–A17, (7) A18–A21 and (8) A22–A25. The range of cross-sectional areas varies from 0.06452 cm^2 to 21.94 cm^2. More information related to the loading conditions and constraints can be found in Kaveh and Talatahari [28].

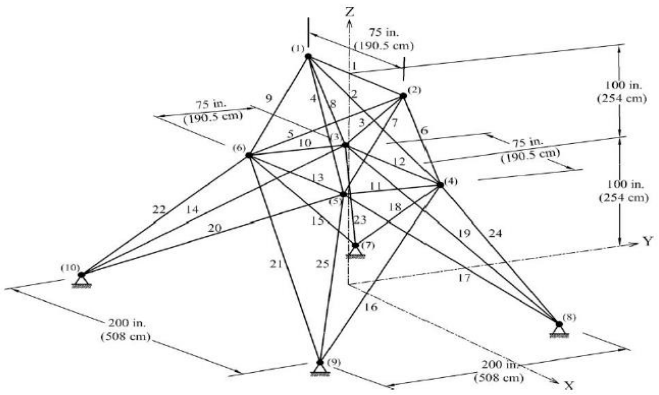

Figure 4. A 25-bar space truss structure

Tables (1-3) list the optimal values of the design variables that are obtained in the present study, in five runs. Also, in Table 4, the results of the best run are compared with those of presented in the literature.

Table 1: Optimum results for 25-bar space truss, using GSA for five sample runs

		Optimal cross-sectional areas (cm²)				
Variable No.	Members	Sample 1	Sample 2	Sample 3	Sample 4	Sample 5
1	A_1	0.1729	0.1910	1.0742	0.0761	1.8464
2	$A_2 \sim A_5$	12.0470	11.5464	12.9032	12.9032	13.5619
3	$A_6 \sim A_9$	20.6831	21.7193	20.6916	19.6793	18.4845
4	$A_{10} \sim A_{11}$	0.4032	1.3187	0.7768	0.2013	0.1013
5	$A_{12} \sim A_{13}$	0.3948	1.0129	0.2026	0.5058	0.0690
6	$A_{14} \sim A_{17}$	3.7219	4.9645	4.2993	5.1058	3.5961
7	$A_{18} \sim A_{21}$	12.0251	13.562	11.6239	11.5077	11.6742
8	$A_{22} \sim A_{25}$	18.1574	15.3464	17.1296	16.8064	19.3548
Weight (kg)		255.644	262.157	256.705	254.968	256.887

Table 2: Optimum results for 25-bar space truss, using ICA for five sample runs

		Optimal cross-sectional areas (cm²)				
Variable No.	Members	Sample 1	Sample 2	Sample 3	Sample 4	Sample 5
1	A_1	0.0645	0.0645	0.0645	0.0645	0.0645
2	$A_2 \sim A_5$	12.8103	12.8909	13.0477	11.0864	13.1497
3	$A_6 \sim A_9$	19.5309	19.9883	18.9303	21.7490	18.5555
4	$A_{10} \sim A_{11}$	0.0645	0.0645	0.0645	0.0645	0.0645
5	$A_{12} \sim A_{13}$	0.0645	0.0645	0.0645	0.0645	0.0645
6	$A_{14} \sim A_{17}$	4.8167	4.1851	4.1090	4.7910	4.4477
7	$A_{18} \sim A_{21}$	11.6522	11.3793	11.8187	12.4026	11.9432
8	$A_{22} \sim A_{25}$	16.9883	17.7251	18.0806	16.2013	17.6542
Weight (kg)		253.513	253.342	253.921	254.584	253.928

Table 3: Optimum results for 25-bar space truss, using ICA-GSA for five sample runs

		Optimal cross-sectional areas (cm²)				
Variable No.	Members	Sample 1	Sample 2	Sample 3	Sample 4	Sample 5
1	A_1	0.065	0.065	0.065	0.099	0.065
2	$A_2 \sim A_5$	12.923	14.148	12.523	20.45	21.09
3	$A_6 \sim A_9$	19.400	17.903	19.580	21.93	21.94
4	$A_{10} \sim A_{11}$	0.065	0.065	0.065	0.56	0.065
5	$A_{12} \sim A_{13}$	0.065	0.065	0.065	0.716	0.065
6	$A_{14} \sim A_{17}$	4.432	4.3806	4.2645	3.26	2.951
7	$A_{18} \sim A_{21}$	10.677	10.419	10.968	18.53	17.53
8	$A_{22} \sim A_{25}$	17.161	17.652	17.264	0.090	1.105
Weight (kg)		247.20	247.68	247.38	253.71	250.05

Table 4: Optimal design comparison for the 25-bar space truss

		Optimal cross-sectional areas (cm²)					
Variable No.	Members	CSS [28]	ICA [29]	CICA-1 [29]	This study GSA	This study ICA	This study ICA-GSA
1	A_1	0.065	0.065	0.065	0.076	0.065	0.0645
2	$A_2 \sim A_5$	12.923	14.148	12.523	12.903	12.891	12.146
3	$A_6 \sim A_9$	19.400	17.903	19.580	19.679	19.988	19.748
4	$A_{10} \sim A_{11}$	0.065	0.065	0.065	0.201	0.0645	0.0645
5	$A_{12} \sim A_{13}$	0.065	0.065	0.065	0.506	0.0645	0.0645
6	$A_{14} \sim A_{17}$	4.432	4.381	4.265	5.106	4.185	4.259
7	$A_{18} \sim A_{21}$	10.677	10.419	10.968	11.508	11.379	11.243
8	$A_{22} \sim A_{25}$	17.161	17.652	17.264	16.807	17.725	16.807
Weight (kg)		247.16	247.68	247.38	254.97	253.34	246.11

All of the statistical values of Table 4 demonstrate that the ICA-GSA in size optimization of 25-bar space truss achieves better performance in comparison to the other algorithms. In addition, Fig. 5 shows the convergence rate of the best run for the ICA-GSA, ICA and GSA algorithms.

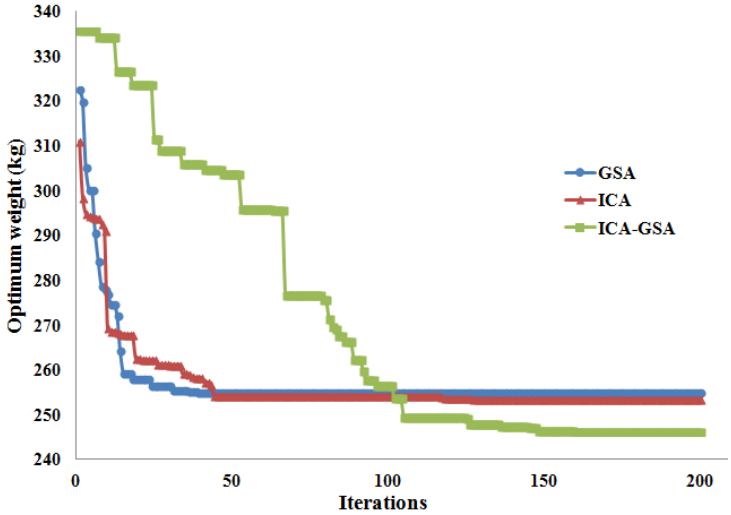

Figure 5. Convergence history of 25-bar space truss

6.2 A 72-bar space truss

For the 72-bar spatial truss structure shown in Fig. 6, the material density is 0.1 lb/in^3 (2767.990 kg/m^3) and the modulus of elasticity is 68,950 MPa. The members are subjected to the stress limits of ±10,000 ksi (±172.375 MPa). The nodes are subjected to the displacement limits of ±0.25 in (±0.635 cm). The 72 structural members of this spatial truss are categorized as 16 groups using symmetry: (1) A1–A4, (2) A5–A12, (3) A13–A16, (4) A17–A18, (5) A19–A22, (6) A23–A30, (7) A31–A34, (8) A35–A36, (9) A37–A40, (10) A41–A48, (11) A49–A52, (12) A53–A54, (13) A55–A58, (14) A59–A66 (15), A67–A70, and (16) A71–A72.

The optimal values of the cross-sectional areas that are achieved in five runs using GSA, ICA and ICA-GSA are presented in Tables (5-7), respectively. Also, in Table 8, the results of the best run are compared with those of presented in [30].

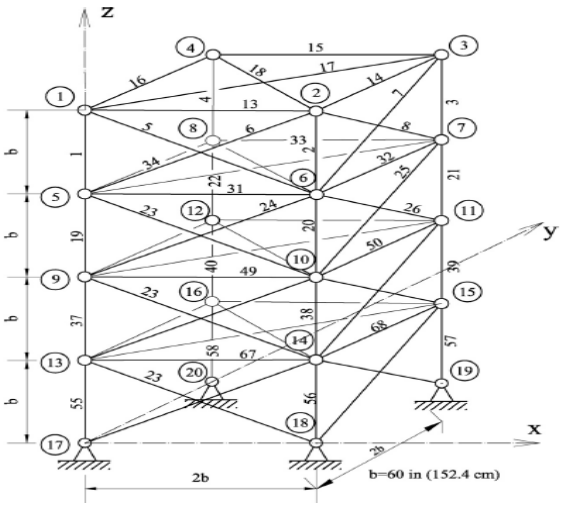

Figure 6. A 72-bar space truss

Table 5: Optimum results for 72-bar space truss, using GSA for five sample runs

		Optimal cross-sectional areas (in²)				
Variable No.	Members	Sample 1	Sample 2	Sample 3	Sample 4	Sample 5
1	A_1~A_4	0.196	0.196	0.141	0.141	0.196
2	A_5~A_{12}	0.391	0.766	0.563	0.766	0.563
3	A_{13}~A_{16}	0.602	0.250	0.563	0.442	0.563
4	A_{17}~A_{18}	0.994	0.563	0.563	0.994	0.994
5	A_{19}~A_{22}	0.442	0.391	0.563	0.785	0.563
6	A_{23}~A_{30}	0.602	0.602	0.563	0.563	0.442
7	A_{31}~A_{34}	0.111	0.111	0.111	0.111	0.111
8	A_{35}~A_{36}	0.111	0.111	0.442	0.111	0.111
9	A_{37}~A_{40}	1.266	1.130	1.130	0.994	0.766
10	A_{41}~A_{48}	0.442	0.602	0.442	0.563	0.563
11	A_{49}~A_{52}	0.111	0.111	0.111	0.111	0.111
12	A_{53}~A_{54}	0.111	0.111	0.111	0.111	0.111
13	A_{55}~A_{58}	2.130	1.800	2.630	1.266	2.130
14	A_{59}~A_{66}	0.602	0.442	0.391	0.442	0.602
15	A_{67}~A_{70}	0.111	0.111	0.111	0.111	0.111
16	A_{71}~A_{72}	0.111	0.111	0.111	0.111	0.111
Weight (lb)		405.370	401.686	402.052	409.215	408.677

Table 6: Optimum results for 72-bar space truss, using ICA for five sample runs

		Optimal cross-sectional areas (in²)				
Variable No.	Members	Sample 1	Sample 2	Sample 3	Sample 4	Sample 5
1	A_1~A_4	0.196	0.196	0.196	0.196	0.196
2	A_5~A_{12}	0.442	0.442	0.442	0.563	0.563
3	A_{13}~A_{16}	0.442	0.563	0.391	0.391	0.442
4	A_{17}~A_{18}	0.602	0.785	0.602	0.563	0.766
5	A_{19}~A_{22}	0.785	0.563	0.442	0.563	0.563
6	A_{23}~A_{30}	0.563	0.442	0.563	0.563	0.442
7	A_{31}~A_{34}	0.111	0.111	0.111	0.111	0.111
8	A_{35}~A_{36}	0.141	0.111	0.111	0.111	0.111
9	A_{37}~A_{40}	1.266	1.228	1.266	1.457	1.457
10	A_{41}~A_{48}	0.563	0.563	0.563	0.563	0.563
11	A_{49}~A_{52}	0.111	0.111	0.111	0.111	0.111
12	A_{53}~A_{54}	0.111	0.111	0.111	0.111	0.111
13	A_{55}~A_{58}	1.620	1.990	2.130	1.800	2.130
14	A_{59}~A_{66}	0.602	0.602	0.563	0.442	0.442
15	A_{67}~A_{70}	0.111	0.111	0.111	0.111	0.111
16	A_{71}~A_{72}	0.111	0.111	0.111	0.111	0.111
Weight (lb)		395.670	396.324	392.026	390.270	394.541

Table 7: Optimum results for 72-bar space truss, using ICA-GSA for five sample runs

		Optimal cross-sectional areas (in²)				
Variable No.	Members	Sample 1	Sample 2	Sample 3	Sample 4	Sample 5
1	A_1~A_4	0.196	0.196	0.196	0.196	0.196
2	A_5~A_{12}	0.602	0.602	0.563	0.563	0.563
3	A_{13}~A_{16}	0.442	0.391	0.442	0.307	0.307
4	A_{17}~A_{18}	0.602	0.563	0.785	0.785	0.563
5	A_{19}~A_{22}	0.785	0.563	0.563	0.766	0.442
6	A_{23}~A_{30}	0.442	0.563	0.563	0.563	0.563
7	A_{31}~A_{34}	0.111	0.111	0.111	0.111	0.141
8	A_{35}~A_{36}	0.111	0.111	0.111	0.111	0.141
9	A_{37}~A_{40}	1.266	1.266	1.457	1.228	1.620
10	A_{41}~A_{48}	0.563	0.442	0.442	0.563	0.442
11	A_{49}~A_{52}	0.111	0.111	0.111	0.111	0.111
12	A_{53}~A_{54}	0.111	0.111	0.111	0.111	0.111
13	A_{55}~A_{58}	1.563	1.800	1.990	1.800	1.990
14	A_{59}~A_{66}	0.563	0.563	0.442	0.442	0.563
15	A_{67}~A_{70}	0.111	0.111	0.111	0.111	0.111
16	A_{71}~A_{72}	0.111	0.111	0.111	0.111	0.111
Weight (lb)		393.284	389.872	391.826	393.149	394.264

Table 8: Optimal design comparison for the 72-bar space truss

Variable No.	Members	ICA [30]	This study		
			GSA	ICA	ICA-GSA
1	A_1~A_4	1.99	0.196	0.196	0.196
2	A_5~A_{12}	0.442	0.766	0.563	0.602
3	A_{13}~A_{16}	0.111	0.250	0.391	0.391
4	A_{17}~A_{18}	0.141	0.563	0.563	0.563
5	A_{19}~A_{22}	1.228	0.391	0.563	0.563
6	A_{23}~A_{30}	0.602	0.602	0.563	0.563
7	A_{31}~A_{34}	0.111	0.111	0.111	0.111
8	A_{35}~A_{36}	0.141	0.111	0.111	0.111
9	A_{37}~A_{40}	0.563	1.130	1.457	1.266
10	A_{41}~A_{48}	0.563	0.602	0.563	0.442
11	A_{49}~A_{52}	0.111	0.111	0.111	0.111
12	A_{53}~A_{54}	0.111	0.111	0.111	0.111
13	A_{55}~A_{58}	0.196	1.800	1.800	1.800
14	A_{59}~A_{66}	0.563	0.442	0.442	0.563
15	A_{67}~A_{70}	0.307	0.111	0.111	0.111
16	A_{71}~A_{72}	0.602	0.111	0.111	0.111
Weight(lb)		392.84	401.686	390. 270	389.872

The values of Table 8 show that the ICA-GSA achieves better performance in comparison to the other algorithms, in size optimization of 72-bar space truss. Also, the convergence rate of the best run for the ICA-GSA, ICA and GSA algorithms are shown in Fig. 7.

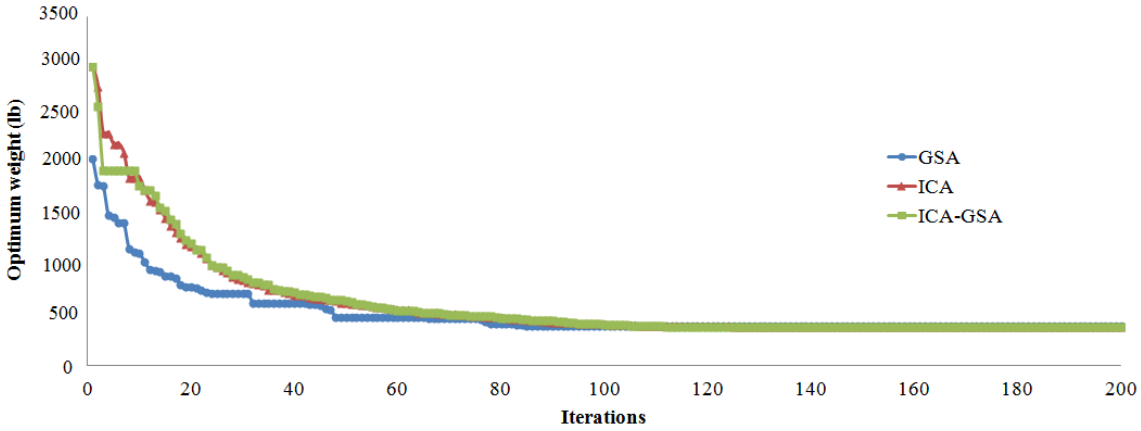

Figure 7. Convergence history of 72-bar space truss

6.3 20×20 double layer grid

A square-on-square double layer grid with 841 nodes (joints) and 3200 members (elements) is presented to examine the proposed optimization method. The depth of the double layer grid is 450 cm and the node spacing in the top and bottom chord is 300 cm (Fig. 8) [21].

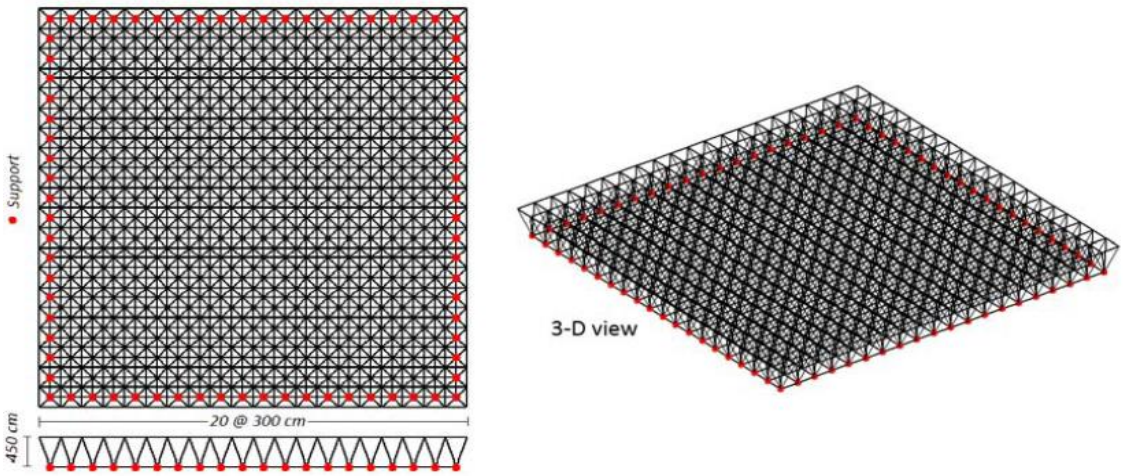

Figure 8. A 20×20 Double layer grid [21]

The assumed material is steel with a Young's modulus and mass density of 2.1×10^6 kg/cm^2 and 7850 kg/m^3, respectively. Also, it is assumed that distributed load on double layer grid is 180 kg/m^2 which are assigned to the nodes of the top grid in the proportion of their load bearing area [21]. The ground structure is considered to be supported at perimeter nodes of the bottom grid. The bottom joints are tabulated in 55 different groups (*NTV* = 55). The number of member types for tensile and compressive members is considered as 3 and 14, respectively, which resulted in 72 design variables [21].

The cross-sectional area of the members is selected from the pipe profiles available in Table 9, where *OD* and *TH* are outer diameter and thickness in centimeter, respectively.

Table 9. Available pipe profiles

No.	*OD*	*T*	No.	*OD*	*T*	No.	*OD*	*T*
1	4.83	0.26	8	13.30	0.40	15	27.30	0.63
2	6.03	0.29	9	13.97	0.40	16	32.39	0.71
3	7.61	0.29	10	15.90	0.45	17	35.56	0.80
4	8.89	0.32	11	16.86	0.45	18	40.64	0.88
5	10.16	0.36	12	19.37	0.45	19	45.72	1.00
6	10.80	0.36	13	21.91	0.45			
7	11.43	0.36	14	24.45	0.63			

This example is optimized in three cases as follows:

Case 1: Topology optimization using GSA.

Case 2: Topology optimization using ICA.

Case 3: Topology optimization using ICA-GSA.

To consider the stochastic nature of the applied optimization approaches, five sample optimization runs are employed for each design case and the achieved optimal solutions in Cases 1, 2 and 3 are presented. Furthermore, it in all of the following figures, the thickness of each element is directly proportional to its cross-sectional area. Also, in these figures, a) through d) denote: double layer grid, top layer, diagonal layer and bottom layer, respectively. It is noted that these obtained configurations are purely for gravity loads and horizontal loads can change the configurations.

In Cases 1, 2 and 3, the optimum topology are shown in Figs. (9, 10 and 11), which the optimum weights of these structures are obtained as 143362 kg, 88504 kg and 80661 kg, respectively.

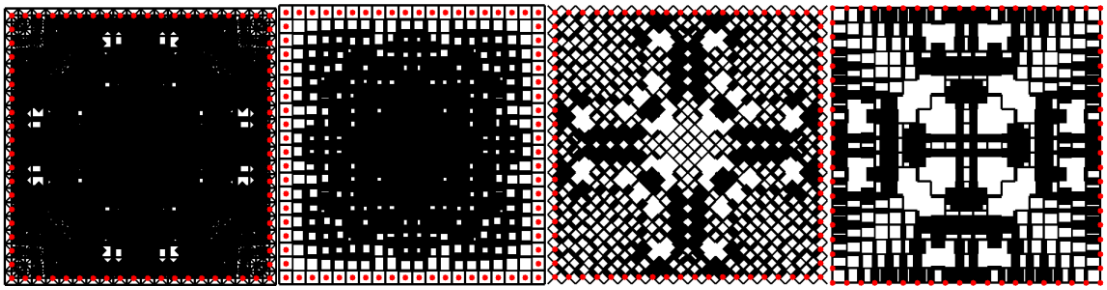

(a) (b) (c) (d)

Figure 9. Optimum topology in Case 1

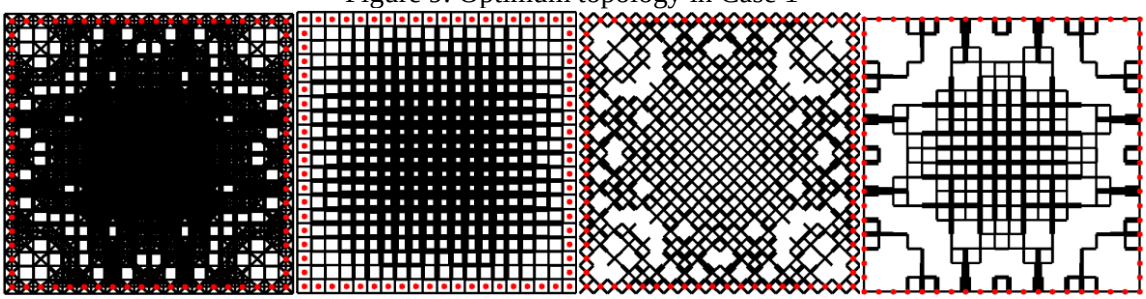

(a) (b) (c) (d)

Figure 10. Optimum topology in Case 2

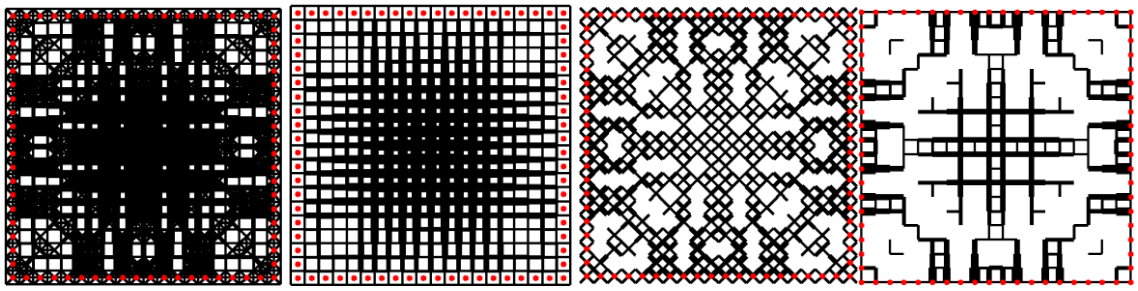

(a) (b) (c) (d)

Figure 11. Optimum topology in Case 3

Table 10: Comparison of the optimum weights of the achieved structures for Cases 1, 2 and 3

Optimum Weight (kg)				
GSA	ICA	ICA-GSA	Topology optimization using ACO [21]	Topology optimization using MMA-ACO [21]
143362	88504	80661	85036	81927

These values validate that ICA-GSA gives better performance than GSA, ICA, ACO and MMA-ACO in topology optimization of double layer grids. Also, Fig. 12 shows the convergence rate of the best obtained topology in Cases 1, 2 and 3.

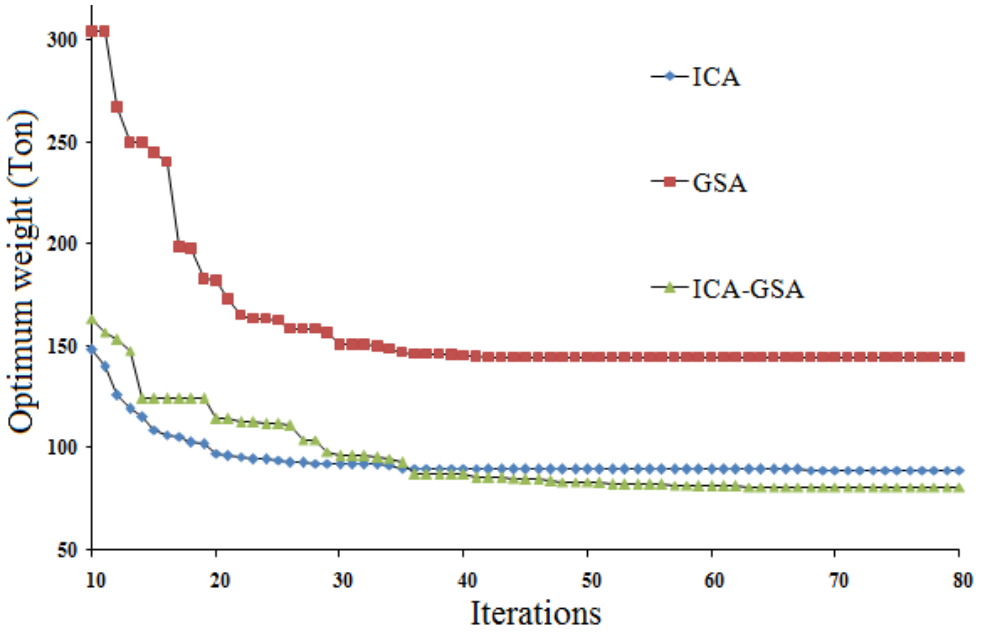

Figure 12. Convergence rate of the best obtained topology using GSA, ICA and ICA-GSA

To have better comparison of ICA-GSA and the other optimization methods, the optimum weights of the obtained topologies for Cases 1, 2 and 3 are listed in Table 11, in which the weights of topologies shown in Figs. (9, 10 and 11) are highlighted. Also, the mean and the standard deviation of these optimum weights are presented in Table 12.

Table 11: Optimum weights of the topologies attained for Cases 1, 2 and 3 for seven sample runs

Case No.	Optimum Weight (kg)				
	sample 1	sample 2	sample 3	sample 4	sample 5
GSA	170503	162439	173214	165540	123362
ICA	88504	90694	89877	89054	92254
ICA-GSA	80601	81854	82589	83652	81973
ACO[21]	89652	89947	89910	85036	92542
MMA-ACO[21]	86152	85607	81927	87648	83116

Table 12: The mean and the standard deviation of the optimum weights

Case No.	$\overline{W}$ (kg)	SD (kg)
GSA	163010	11758
ICA	90077	1473
ICA- GSA	82146	1093
ACO[21]	89417	2717
MMA-ACO[21]	84899	2312

These values validate that the ICA-GSA achieves better performance than the GSA, ICA, ACO and MMA-ACO in topology optimization of large scale skeletal structures. It is noted that in (Mashayekhi *et al*. 2012) to obtain better cross-sectional areas for optimum achieved topologies, at the end of the first phase of the topology optimization, the local search space of the following phases is applied by the neighborhood of the previous elitist ant's solution, with 100 ant's, and the size optimization of the obtained optimum topology is implemented in several phases until the optimum weight of the structure is not changed significantly in two successive phases. But in this article, the optimum topology is achieved only in one phase with 50 countries and 80 iterations, which is significant. In addition, the maximum and the allowable amount of displacement of the structure are shown in Table 13. These values indicate that the displacement of the structure is not an active constraint.

Table 13: Maximum and allowable displacement

Maximum Displacement (cm)			Allowable Displacement (cm)
GSA	ICA	ICA-GSA	
6.6693	10.3033	10.0601	15.833

Also, the maximum and the allowable amounts of the internal stress of members are shown in Table 14 and these obtained values using GSA, ICA and ICA-GSA are schematically shown in Figs. 13, 14 and 15, respectively.

Table 14: Maximum and allowable amounts of the internal stress of members (kg/cm²)

GSA		ICA		ICA-GSA	
Allowable stress	Maximum stress	Allowable stress	Maximum stress	Allowable stress	Maximum stress
907.23	334.19	525.19	285.17	401.65	285.41
525.19	470.94	967.77	275.90	525.19	460.51

1070.78	582.63	825.68	455.96	667.21	632.95
825.68	661.96	1207.47	399.85	825.68	646.67
1141.97	850.00	1162.15	755.31	825.68	709.34
1141.97	840.85	1207.47	670.45	1162.15	860.67
1207.47	736.71	1290.16	529.57	1141.97	998.39
1207.47	947.46	1207.47	892.74	1141.97	1098.01
1207.47	1099.11	1225.74	965.11	1207.47	1018.92
1207.47	1182.85	1309.26	568.62	1207.47	1137.98
1225.74	1207.32	1290.16	932.56	1225.74	1174.24
1263.00	1138.80	1290.16	1079.39	1263.00	1127.41
1263.00	1235.04	1290.16	1018.76	1263.00	1241.01
1290.16	1251.94	1309.26	857.90	1290.16	1153.59
1440	1152.01	1440	763.01	1440	1138.21
1440	1422.28	1440	977.68	1440	1298.56
1440	1248.10	1440	611.38	1440	1356.43

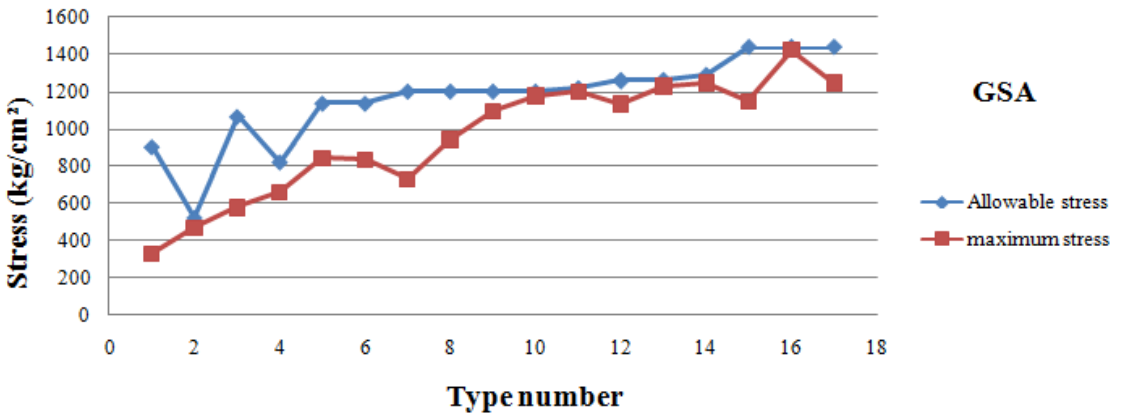

Figure 13. Maximum and allowable amounts of the internal stress of members, using GSA

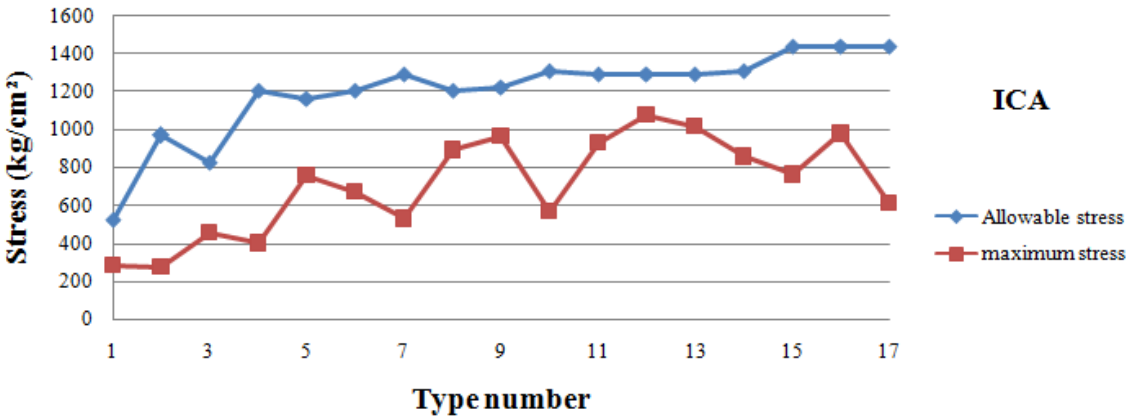

Figure 14. Maximum and allowable amounts of the internal stress of members, using ICA

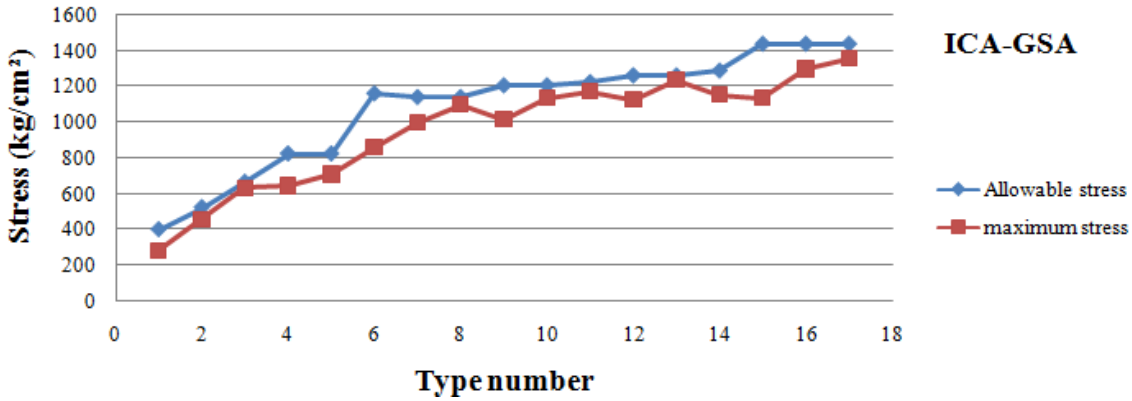

Figure 15. Maximum and allowable amounts of the internal stress of members, using ICA-GSA

7. CONCLUSIONS

In this article, an efficient optimization method has been introduced by combination of ICA and GSA for topology optimization of double layer grids. The present combined method, ICA-GSA, was based on ICA but it used the law of gravity of GSA to move countries toward their relevant imperialist. The proposed method was applied for topology optimization of a large-scale double layer grid, and the optimization was implemented in three cases. In the solved example, the following numerical results can be drawn as:

(a) In comparison with other heuristic algorithms, the ICA-GSA method has better performance than ICA, CSS, CICA and GSA in the size optimization of the space trusses.

(b) ICA method finds better answer in the topology optimization of large scale skeletal structures than those of optimum topologies attained by GSA.

(c) ICA-GSA method obtains the optimum topologies with lower weight than those of optimum topologies achieved by ICA, GSA, ACO and MMA-ACO.

(d) In ACO and MMA-ACO to achieve a better solution, at the end of the first phase of topology optimization, the local search space of the following phases is applied by the neighborhood of the previous elitist ant's solution, with 100 ants, and the size optimization of the obtained optimum topology is implemented in several phases. But ICA-GSA gives the optimum topology only in one phase with 50 countries and 80 iterations. Therefore, ICA-GSA approach is more reliable than ACO and MMA-ACO, in the topology optimization of large-scale skeletal structures.

REFERENCES

1. Kicinger R, Arciszewski T, De Jong K. Evolutionary computation and structural design: A survey of the state-of-the-art, *Comput Struct* 2005; **83**: 1943-78.
2. Deb K, Gulati S. Design of truss-structures for minimum weight using genetic algorithms, *Finite Elem Anal Des* 2001; **37**: 447-65.

3. Imai K, Schmith LA. Configuration optimization of trusses, *J Struct Div* 1981; **5**(107):745-56.
4. Ringertz UT. On topology optimization of trusses, *Eng Optim* 1985; **9**: 209-18.
5. Kirsch U. Optimal topologies of truss structures, *Comput Method Appl Mech Eng* 1989; **72**: 15-28.
6. Wang D, Zhang WH, Jiang JS. Combined shape and sizing optimization of truss structures, *Comput Mech* 2002; **29**(4**-**5): 307-12.
7. Ringertz UT. A branch and bound algorithm for topology optimization of truss structures, *Eng Optim* 1986; **10**: 111-24.
8. Hajela P, Lee E. Genetic algorithms in truss topological optimization, *Int J Solids Struct* 1995; **22**(32): 3341-57.
9. Tang WY, Tong LY, Gu YX. Improved genetic algorithm for design optimization of truss structures with sizing, shape and topology variables, *Int J Numer Meth Eng* 2005; **62**: 1737-62.
10. Fourie PC, Groenwold AA. The particle swarm optimization algorithm in size and shape optimization, *Struct Multidiscip Optim* 2002; **23**: 259-67.
11. Lamberti L. An efficient simulated annealing algorithm for design optimization of truss structures, *Comput Struct* 2008; **86**: 1936-53.
12. Kaveh A, Farmhand B, Talatahari S. Ant colony optimization for design of space trusses, *Int J Sp Struct* 2008; **3**(23): 167-81.
13. Luh GC, Lin CY. Optimal design of truss structures using ant algorithm, *Struct Multidiscip Optim* 2008; **36**: 365-79.
14. Sonmez M. Artificial bee colony algorithm for optimization of truss structures, *Appl Soft Comp* 2011; **11**: 2406-18.
15. Kawamura H, Ohmori H, Kito N. Truss topology optimization by a modified genetic algorithm, *Struct Multidiscip Optim* 2002; **23**: 467-72.
16. Grieson DE, Pak WH. Optimal sizing, geometrical and topological design using a genetic algorithm, *Struct Optim* 1993; **6**: 151-9.
17. Ohsaki M. Genetic algorithm for topology optimization of trusses, *Comput Struct* 1995; 2(**57**): 219-25.
18. Su RY, Gui LJ, Fan ZJ. Truss topology optimization using genetic algorithm with individual identification technique, *Proceedings of the World Congress on Engineering*, Vol. II, WCE, London, UK, 2009.
19. Rozvany GIN. Difficulties in truss topology optimization with stress, local buckling and system stability constraints, *Struct Optim* 1996; **11**: 213-17.
20. Parke G, Disney P. Space Structures 5. Thomas Telford, London, 2002.
21. Mashayekhi M, Salajegheh E, Salajegheh J, Fadaee MJ. Reliability-based topology optimization of double layer grids using a two-stage optimization method, *Struct Multidiscip Optim* 2012; 45(**6**): 815-33.
22. Mashayekhi M, Fadaee MJ, Salajegheh J, Salajegheh E. Topology optimization of double layer grids for earthquake loads using a two-stage ESO-ACO method, *Int J Optim Civ Eng* 2011a; **2**(1): 211-32.

23. Mashayekhi M, Salajegheh J, Fadaee MJ, Salajegheh E. A two-stage SIMP-ACO method for reliability-based topology optimization of double layer grids, *Int J Optim Civ Eng* 2011b; **1**(4): 521-42.
24. Kang BS, Park GJ, Arora JS. A review of optimization of structures subjected to transient loads, *Struct Multidiscip Optim* 2006; **31**: 81-95.
25. Rashedi E, Nezamabadi-pour H, Saryazdi S. GSA: a gravitational search algorithm, *Inf Sci* 2009; 179(**13**): 2232-48.
26. Atashpaz-Gargari E, Lucas C. Imperialist competitive algorithm: An algorithm for optimization inspires by imperialistic competition, *IEEE Congress on Evolutionary Computation*, Singapore, 2007.
27. Kaveh A, Talatahari S. Imperialist competitive algorithm for engineering design problems, *Asian J Civ Eng* 2010; **11**(6): 675-97.
28. Kaveh A, Talatahari S. Optimal design of skeletal structures via the charged system search algorithm, *Struct Multidiscip Optim* 2010; **41**(6): 893-911.
29. Talatahari S, Kaveh A, Sheikholeslami R. Chaotic imperialist competitive algorithm for optimum design of truss structures, *Struct Multidiscip Optim* 2012; **46**(3): 355-67.
30. Kaveh A, Talatahari S. Optimum design of skeletal structures using imperialist competitive algorithm, *Comput Struct* 2010; **88**: 1220-9.